Homogenization method for a discrete-continuum simulation of dislocation dynamics

Article *in* Journal of the Mechanics and Physics of Solids · September 2001

DOI: 10.1016/S0022-5096(01)00026-6

CITATIONS
74

READS
65

3 authors, including:

Benoit Devincre
French National Centre for Scientific Research
111 PUBLICATIONS **3,791** CITATIONS

SEE PROFILE

Ladislas Kubin
The French Aerospace Lab ONERA
257 PUBLICATIONS **8,447** CITATIONS

SEE PROFILE


PERGAMON

Journal of the Mechanics and Physics of Solids
49 (2001) 1969–1982

JOURNAL OF THE
MECHANICS AND
PHYSICS OF SOLIDS

www.elsevier.com/locate/jmps

Homogenization method for a discrete-continuum simulation of dislocation dynamics

C. Lemarchand, B. Devincre, L.P. Kubin *

LEM, CNRS-ONERA (OM), BP 72, 29 Av. de la Division Leclerc, 92322 Châtillon Cedex, France

Abstract

The question of the description of the elastic fields of dislocations and of the plastic strains generated by their motion is central to the connection between dislocation-based and continuum approaches of plasticity. In the present work, the homogenization of the elementary shears produced by dislocations is discussed within the frame of a discrete-continuum numerical model. In the latter, a dislocation dynamics simulation is substituted for the constitutive form traditionally used in finite element calculations. As an illustrative example of the discrete-continuum model, the stress field of single dislocations is obtained as a solution of the boundary value problem. The hybrid code is also shown to account for size effects originating from line tension effects and from stress concentrations at the tip of dislocation pile-ups.

Keywords: Homogenization; Plastic strain; A. Dislocation dynamics; C. Finite elements; Size effects

1. Introduction

In the last decade the traditional constitutive forms employed in continuum approaches of plasticity have been improved to include the slip geometry and, further, the temporal evolution of spatially averaged dislocation densities (see for instance Estrin, 1996; Cuitiño and Ortiz, 1992; Tabourot et al., 1997). Although these formulations may include characteristic lengths stemming from dislocation properties, their output still has no length scale. More recently, new models have appeared that aim at describing size effects and non-uniform plastic flow by incorporating non-local forms and scaling lengths by different methods and with various justifications (see, among others, Aifantis, 1984; Fleck et al., 1994; Acharya and Bassani, 2000). As far as dislocation

* Corresponding author. Tel.: +33-1-4673-4441; fax: +33-1-4673-4155.
E-mail address: ladislas.kubin@onera.fr (L.P. Kubin).

0022-5096/01/$ - see front matter
PII: S0022-5096(01)00026-6

processes are concerned, these attempts are still missing dislocation properties that are thought by metallurgists to be essential for a physically based description of plastic flow.

Simulations can be helpful to bypass these theoretical limitations and to provide objective guidelines for the modeling of plastic deformation. Such numerical models make use of a discrete description of the dislocation dynamics, combined with a finite element (FE) calculation of the boundary value problem. Since a coupling is established between discrete and continuum descriptions of plasticity, the question of the homogenization of the properties of dislocations cannot be eluded. This point was first considered by Cleveringa et al. (1997a, b) in the case of a model composite material. The 2-D method used by Cleveringa et al., as well as further 3-D models by Fivel et al. (1998) and Fivel and Canova (1999), make use of the superposition principle. The solution of the boundary value problem is obtained as the sum of two contributions. The first represents the solution for dislocations in an unbounded continuum and the other is the complementary elastic solution needed to satisfy equilibrium at external and internal boundaries. The last contribution is computed by a FE code.

In the present work, we make use of a hybrid 3-D discrete-continuum model (DCM) that includes within a FE code a mesoscopic dislocation dynamics (DD) simulation replacing the usual constitutive form. It is important to note that the DCM does not make use of the superposition principle. Instead, it aims at computing equilibrium conditions both inside the considered volume and at its external or internal interfaces. As a consequence it is no longer necessary to make use of analytical expressions for the dislocation self-stress fields. As will be shown below, the definitions of the local plastic shears induced by the motion of individual dislocations and their homogenization have then to be treated with great care. This problem actually stands at the core of the connection between the two codes, since the plastic strains constitute the basic information transmitted from the DD simulation to the FE simulation. The DCM is briefly described in Section 2 and the homogenization of the dislocation fields is discussed in Section 3. This leads to the definition of an adequate homogenization dimension. Then, the DCM is applied to the examination of the fields of single dislocation configurations. To illustrate the fact that the DCM includes a length scale, it is applied in Section 5 to the study of two basic size effects stemming from the interactions of dislocations with interfaces, respectively, the confinement effect and the pile-up effect. Concluding remarks are presented in Section 6.

2. The discrete-continuum model (DCM)

The DCM is composed of two coupled codes. On the one hand, a three-dimensional DD code solves the dynamics and local reactions of discrete dislocation lines and computes the plastic strain generated by dislocation glide. On the other hand, a FE code computes the displacement field that is solution of the boundary value problem, making use of the plastic strain field yielded by the DD simulation. Thus, the DD code serves as a substitute for the constitutive form used in usual FE frameworks. The coupling procedure, which is described below, involves two important steps. First,

the stresses defined at the nodes of the FE mesh are calculated at the positions on the dislocation lines where the dynamics is computed. Next, the discrete plastic shears produced by the motion of dislocation segments are transformed into local strains and transferred to the FE mesh. The first operation is an interpolation procedure, whereas the second one is a homogenization procedure.

The DD simulation used in the DCM calculations has been described in several publications (Devincre, 1995; Devincre and Kubin, 1997; Kubin and Devincre, 1999). For the present purposes, it is sufficient to mention that this mesoscopic simulation code solves the equation of motion of dislocation segments whose line curvature is discretized. In addition, this simulation includes a set of local rules that account for the core properties of the dislocations, typically their stress vs. velocity relationship and cross-slip properties, and for the contact reactions occurring when dislocations cross each other. Quite generally, the main limitation of DD simulations stems from the long-range character of the dislocation stress fields. Hence, the computation of elastic interactions of dislocation segments, whose number increases with plastic strain, is an $O(N^2)$ problem. Although algorithms have been developed that can reduce this computational task (cf. e.g. Verdier et al., 1998), the latter constitutes a bottleneck that drastically restricts the dimension of the simulated volumes. In addition, numerically efficient formulations for the stress fields of dislocation segments are only available for the case of an isotropic, infinite medium. As a consequence, the boundary conditions cannot be implemented rigorously. In practice, it is generally assumed that the loading conditions induce uniform applied stresses inside the simulated volume. At the external surfaces, strong approximations have to be made to account for the conditions of mechanical equilibrium, both in the case of small single crystals and when periodic boundary conditions are used.

The hybrid DCM method has been briefly discussed by Lemarchand et al. (1999, 2000). It is based on a coupling between the DD code and a FE code (ZéBuLon), each code functioning with its own time step (typically 10^{-9} s for the DD code and 10^{-8} s for the FE code). In short, the FE code is used to mesh the simulated volume and periodically test the conditions of mechanical equilibrium. The FE part of the DCM operates in a conventional manner except that, at simulation step n, the increments of total deformation, $\delta\underline{\underline{\varepsilon}}^{\mathrm{t}}_n$, are computed simultaneously at all the Gauss points of the FE mesh. From the plastic strain solutions at the last DD step, $\underline{\underline{\varepsilon}}^{\mathrm{p}}_{n-1}$, the stresses at step n are defined at the Gauss points using an explicit scheme:

$$\underline{\underline{\sigma}}_n = C(\underline{\underline{\varepsilon}}^{\mathrm{t}}_n - \underline{\underline{\varepsilon}}^{\mathrm{p}}_{n-1}), \tag{1}$$

where C is the tensor of elastic moduli. Note that knowledge of stresses everywhere in the FE mesh is necessary at the beginning of each time step because the latter serve as input for solving the dynamics of the dislocation in the discrete part of the model. More precisely, the stresses at the Gauss points of the FE mesh are interpolated to the midpoint of the dislocation segments, where the Peach–Koehler force has to be defined to solve dislocation motion. Once this force is estimated on all the dislocation segments, one plastic step is performed by the mesoscopic code.

The stress interpolation procedure is split into two sub-steps. First, the stresses defined at the Gauss points are transformed into nodal stresses by making use of

pseudo-inverse functions, i.e., inverse functions of the shape functions that are associated with the type of element used in the FE mesh. Such nodal stress values are common to several neighboring elements. Hence, to avoid stress jumps when a dislocation segment crosses the boundary of a mesh element, an average stress value is defined at each node. The second step consists of interpolating these stresses on the dislocation segments, making use of the set of polynomial forms associated with the type of element used to mesh the simulated continuum. Of course, the quality of this interpolation is directly related to the flexibility offered by this set in terms of number and order of the polynomials. For this reason, it is preferable to make use of mesh elements containing a large number of nodes.

The above stress field interpolation allows performing DD steps. During the latter, the motion of the dislocation segments produces discrete shears in a finite number of glide planes. These discrete strains have to be somehow transferred at the Gauss points to define the plastic strain that will serve as input for the next FE step. This important homogenization procedure will be discussed in detail in the next section. When $\varepsilon_n^{\mathrm{p}}$ is known, the conditions of mechanical equilibrium are tested with the FE code and, if necessary, the whole procedure described above is iterated until a prescribed level of convergence is met. The number of iterations needed at each step of DCM depends on the complexity of the investigated configuration, on the amplitude of the time or deformation increment tested and the type of FE mesh element used. As an example, the number of iterations performed in the illustrations shown below is always smaller than five.

Although the DCM procedure includes some technicalities, it is transparent in physical terms. In contrast with the traditional constitutive formulations, the present model incorporates, at least in principle, all the defect properties needed for a physical description of plastic properties, including the relevant microstructural length scales. Further, the stress fields of the dislocation segments is no longer an input property of the DD code, as it is part of the global solution of the boundary value problem. Thus, the computation of the stress on dislocation segments being interpolated from a constant number of nodes, the calculation of the dislocation–dislocation elastic interaction is no longer an $\mathrm{O}(N^2)$ problem. Finally, one may notice that taking into account the long-range character of the dislocation fields is somehow equivalent to making use of a non-local constitutive form. The DCM has, however, limitations of its own, as will be discussed in the concluding part.

3. Homogenization procedure

Before coming to the homogenization process, it is necessary to describe how the initial configurations are constructed. By definition, dislocations are the defects that ensure the compatibility between slipped and non-slipped areas in a crystal. Quite generally, their stress field can be calculated via a Volterra-like process, as discussed by Mura (1993). This process consists of introducing a dislocation line from the external surface and moving it in position by glide (cf. Fig. 1). The initial conditions for a deformation step in the DCM, including the first step, are implemented in the same

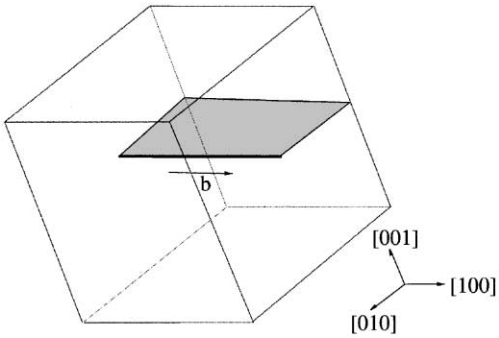

Fig. 1. Introduction of a dislocation line in the DCM, here a screw of Burgers vector [1 0 0], by a Mura process.

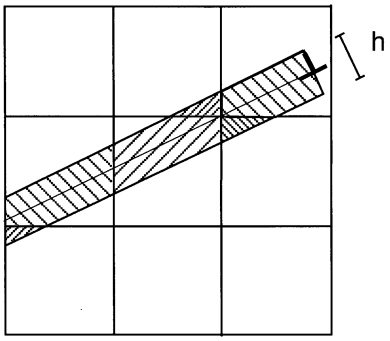

Fig. 2. Schematic view of the sheared volume associated with dislocation glide. The hatched areas represent the portions of the sheared volume enclosed within successive volume elements of the Gauss points in the FE mesh.

manner. Hence, the stress field of a dislocation is not derived from the actual position of its line but from the slipped area due to its previous motion. This elementary dislocation slip, whose direction and amplitude is given by the Burgers vector $\underline{b}$, is physically localized in one crystallographic slip plane and bounded by a singularity at the dislocation line. As it is, such a configuration is not suited for a continuum calculation and has to be homogenized.

The homogenization procedure is based on the concept of local average and can be decomposed into two steps. First, it is assumed that the elementary slip events associated with the motion of dislocations in their glide plane can be extended over a slab of finite thickness h (cf. Fig. 2). This is formally equivalent to replacing the real dislocations by a continuum distribution of parallel infinitesimal dislocations moving along a thin ribbon normal to the glide plane. Such distributions reproduce well the elastic fields of real dislocations outside the sheared volume (Kroupa, 1994; Saada and Shi, 1995). It was shown by Eshelby (1966) that this procedure is formally equivalent to replacing the dislocation line by a disclination dipole of height h. The second step

consists in redistributing these homogenized amounts of slip, which are now tensorial plastic shears, at the Gauss points of the FE mesh. This is performed with the help of Orowan's law. Defining by $\Delta\gamma_n^{i,s}$ the plastic shear increment produced in the elementary volume V_G associated to each Gauss point by a dislocation segment (i) belonging to the slip system (s) of Burgers vector $\underline{b}^s$, we have

$$|\Delta\gamma_n^{i,s}| = \frac{(|b_i|/h)\Delta V_s}{V_G}, \tag{2}$$

where ΔV_s is the volume of the intersection between the sheared slab and the elementary volume, V_G (cf. Fig. 2). Then, the increment of total plastic strain measured at the Gauss points is the sum of the contributions from all the dislocation segments on all the active slip systems that intersect their elementary volume:

$$\underline{\underline{\Delta\varepsilon_n^p}} = \sum_s \sum_i |\Delta\gamma_n^{i,s}| (\underline{\ell}_s \otimes \underline{n}_s)^{sym}, \tag{3}$$

each slip system s being defined by its unit shear direction $\underline{\ell}_s = \underline{b}_s/|\underline{b}_s|$ and the unit normal $\underline{n}_s$ to its glide plane.

The question of the dimension of the homogenization parameter, h, is a key point. Indeed, increasing the value of h induces a progressive smearing out of the dislocation elementary slip and, therefore, leads to increasing inaccuracies in the calculation of the elastic stress and strain fields close to the dislocation line. The optimum solution then consists in selecting the smallest value compatible with the type of elements used and the crystallography of the considered material. This point can be discussed from Fig. 3 where calculations of the homogenized plastic shear strain are shown for a dislocation gliding in a $\{1\,0\,0\}$ slip plane and in a plane of arbitrary orientation with respect to the FE mesh. The orientation selected here, $\{0\,1\,2\}$, is a rather unlikely one, but is well suited for illustrating the influence of slip geometry.

The homogenization parameter is first set to the value $h = b$, in order to reproduce the shearing of a single atomic plane. As shown in Fig. 3a, a uniform homogenized shear is recorded at the Gauss points, the $\{1\,0\,0\}$ slip plane being parallel to the rows of Gauss points. In contrast, with a slip plane non-parallel to the FE mesh, neighboring volume elements can see very different homogenized shears (cf. Fig. 2, above). This considerably disturbs the FE solution, as can be seen from Fig. 3b where a periodic succession of small and large shears is obtained. By increasing the homogenization height (cf. Fig. 3c), a uniform plastic shear is again obtained. A typical value of h that scales with the dimension L of the mesh elements (here $h = 3L/2$, see below for further discussion), was found to lead to correct results for all the tested slip geometries.

Another important technical point resides in the selection of the most suited type of mesh element. In agreement with the standard FE framework (Bathe, 1996), it was found that elements leading to reduced order numerical integration should be preferred. Indeed, such elements avoid overestimating the structural stiffness arising from the meshing procedure. For this reason, quadratic elements with 20 nodes and 8 G points have been used in most of the present calculations.

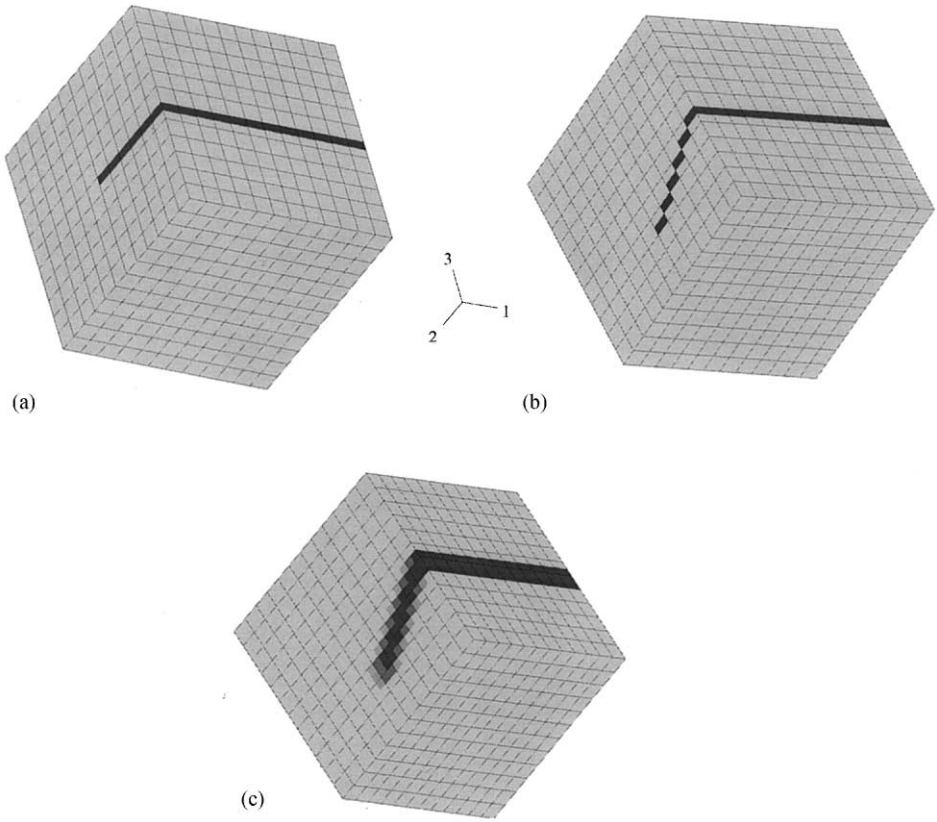

Fig. 3. Isovalues of the plastic strain at the Gauss points due to the motion of a screw dislocation of Burgers vector [1 0 0] during the process shown in Fig. 1. The linear dimension of the simulation cube is 15 μm. The FE mesh is made up of $12^3 = 1728$ cubic elements of dimension L with 20 modes and 8 G points. (a) (0 0 1) slip plane with a homogenization height $h = b$. The distance between the rows of Gauss points being $L/2$, a uniform shear is obtained over a slab of thickness $L/2$. (b) (0 1 2) slip plane with $h = b$. The homogenized shear is no longer uniform. (c) (0 1 2) slip plane with $h = 3L/2 = 3676b$. The homogenized shear is uniform.

4. Stress field of single dislocations

Results obtained with the homogenization procedure defined above are illustrated in the case of single edge and screw dislocations in a crystal of finite dimension. The dislocations are introduced from the side of the crystal of linear dimension 15 μm and brought to the center of the crystal. The FE computations are performed in the same conditions as those of Fig. 3a.

The computed displacement fields at equilibrium are illustrated in Figs. 4a and b by their component parallel to the Burgers vector. This component is magnified by a factor of 3000, which allows recognizing easily known features such as, for the

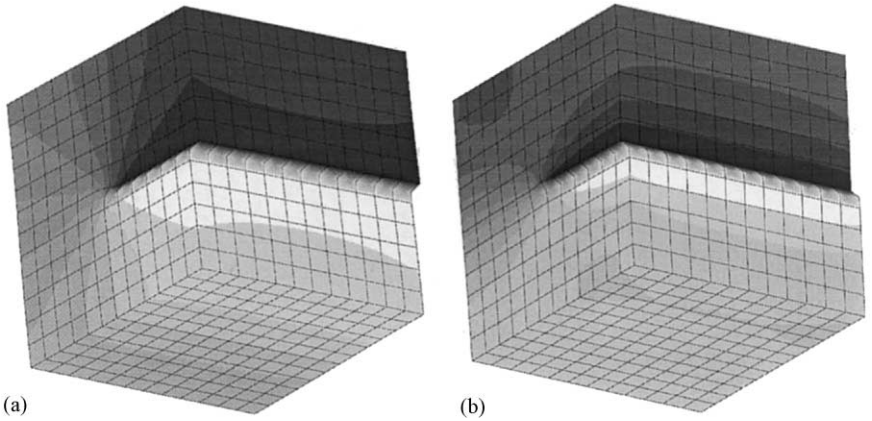

Fig. 4. Isovalues of the component of the displacement field parallel to the Burgers vector superimposed to the deformed crystal for (a) a screw dislocation of Burgers vector [1 0 0] gliding in a (0 0 1) plane, (b) an edge dislocation of line direction [1 0 0] and Burgers vector [0 1 0] gliding in a (0 0 1) plane. The displacements are magnified by a factor of 3000 for better visualization (the gray scale goes from white to black for displacement going from 0 to b).

screw dislocation, the transformation of the (1 0 0) planes into a helicoidal surface (cf. Fig. 4a). These computations were performed within an elastically isotropic frame, in order to facilitate comparisons with the classical elastic solution, taking copper ($\mu = 42$ GPa, $\nu = 0.33$) as a model material. In Fig. 5, the computed stress component σ_{13} of the screw dislocation is plotted as a function of the radial distance d to the line. It is compared to the analytical solution for a single dislocation bounded by four image dislocations, which provides a first order approximation for the exact solution. At distances $d > L$, the agreement is excellent. One can see that, in conformity with the discussion of the homogenization procedure given in Section 3, the dislocation core is extended and the elastic singularity is smeared out by the interpolation procedure. Thus, at approach distances smaller than the dimension of a FE mesh, the interpolation procedure fails to yield the correct stress value.

For the stress field of the edge dislocation, the computation was performed using anisotropic elastic coefficients of cubic symmetry, still in the case of copper ($C_{11} = 166.1$ GPa, $C_{12} = 119.5$ GPa, $C_{44} = 151.2$ GPa), the anisotropy coefficient of which is $A = 3.21$. Isovalues of the non-zero components of the stress tensor are shown in Fig. 6. These results do not strongly differ from the isotropic solutions. Far from the surface of the simulated crystal and for distances to the line larger than the mesh dimension, they also fully agree with the rather complex solutions yielded by the elastic theory of dislocations.

5. Length scales and size effects

A dislocation line blocked under stress between two obstacles separated by a distance ℓ bows out and further recovers its mobility when a critical resolved stress value τ_c is

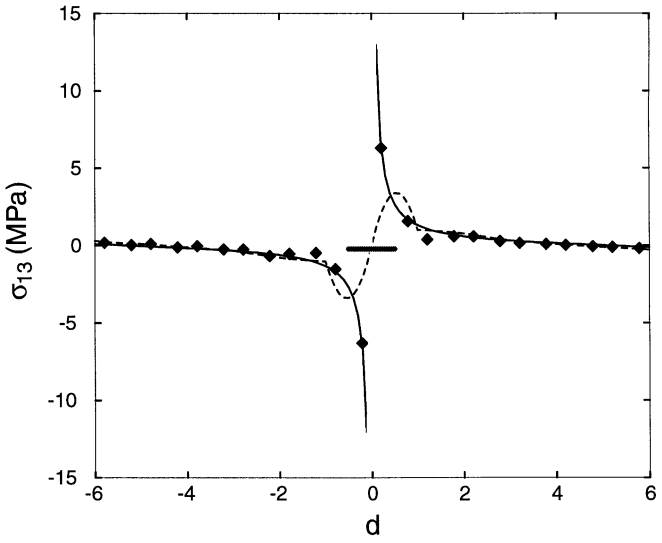

Fig. 5. The radial stress component of a [1 0 0] screw dislocation, σ_{13}, as measured at the Gauss points (data points), vs. the distance d to the dislocation line. The full line shows a first order theoretical solution for a screw dislocation in the same bounded medium. The dotted line shows the stress values calculated from nodal averaged values. The homogenization distance $h = L/2$ is indicated by a horizontal bar.

reached locally. In isotropic elasticity and within the approximation of the local line tension one has

$$\tau_c = 2\beta \frac{\Gamma}{b\ell} \approx 2\beta \frac{\mu b}{\ell}, \tag{4}$$

where $\Gamma \approx \mu b^2$ is the line tension of the dislocation and β a parameter that quantifies the strength of the obstacle ($\beta \leqslant 1$). Eq. (4) applies to many different situations, depending on the nature of the obstacle, and leads to simple scaling relations. When the average length of the dislocation lines, ℓ, is governed by one specimen dimension, a size effect arises. Measuring the critical stresses for such effects is a benchmark for DD simulations (Gómez-García et al., 1999). A check of these scaling relations and size effects has been performed with the help of the DCM. The line tension properties of dislocations are incorporated into the DD part of the hybrid code, in a form more sophisticated than that of Eq. (4) but still within the local line tension formulation (see Gómez-García et al. (1999) for more detail). An additional non-local contribution arises from the elastic interactions of the segments used to discretize a curved dislocation line. This contribution is computed by the FE part of the DCM code.

We consider first the critical stress, τ_{FR} for the operation of a Frank–Read source. In such a case, the obstacles to dislocation motion are strong ones and $\beta \approx 1$ in Eq. (4). The non-local contribution typically is of the order of 0.1–$0.15\tau_{FR}$ for segment lengths in the micrometer range (Devincre and Condat, 1992). In order to reproduce exactly this critical stress, the FE mesh must be small enough so that details of the line curvature can be taken into account. This concerns, in particular, the elastic interactions

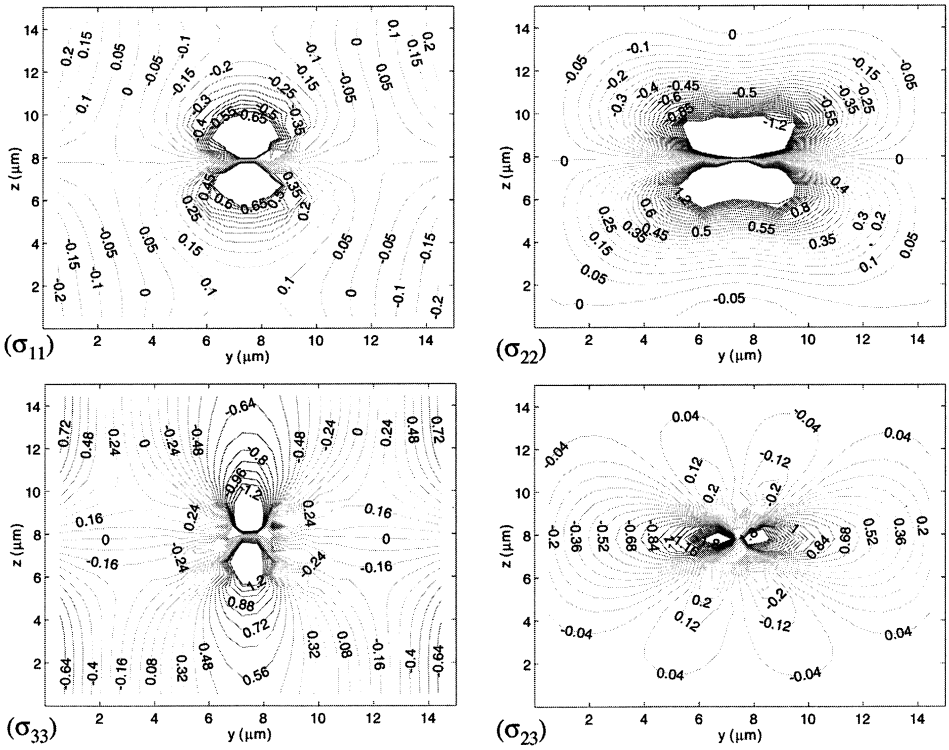

Fig. 6. Same edge dislocation as in Fig. 4b. Isovalues for the non-zero components of the stress tensor. Close to the dislocation line, the isostress values are too dense to be drawn.

of the different segments describing the bowed out line. As a result, the mesh dimension L has to be adjusted to the considered configuration. In the present case, it was checked that for a dislocation source of initial length ℓ, the expected value of the Frank–Read stress is exactly reproduced provided that $L \leqslant \ell/4$. For instance, for a source of initial length 0.1 μm in copper, the DCM yields $\tau_{FR} = 106$ MPa, to be compared with the value yielded by the DD simulation, $\tau_{FR} = 104$ MPa. The small difference can be attributed to the boundary conditions: the DD code makes use of the dislocation fields in infinite media, whereas a single crystal of linear dimension 0.3 μm was simulated using the DCM. This adaptation of the meshing to the configuration investigated is intrinsic to the coupled DCM and stems from the nature of the homogenization process. Indeed, the proper description of any intrinsic length scale, here the initial length of the dislocation source, requires an adequate refinement of the FE mesh.

A confinement size effect is observed in thin channels, when the distance between two parallel and impenetrable boundaries limit the lateral expansion of the dislocation loops, and in free-standing epitaxial layers. This last case is illustrated by Fig. 7, which shows the critical stress for the motion of an edge dislocation as a function of the thickness H of the layer. The dislocation has the same crystallographic features as

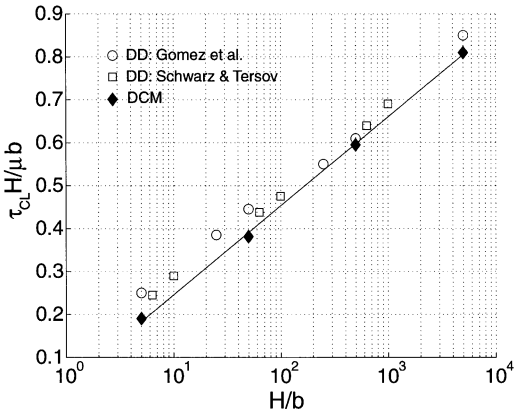

Fig. 7. Critical stress (in reduced units) for the motion of an edge dislocation in a free-standing film deposited on a substrate vs. the reduced film thickness H/b. The slip plane of the dislocation is perpendicular to the interface. The data shown include: (♦) Values obtained using the DCM. The thin foil is meshed with $15 \times 15 \times 5$ elements. It rests on a substrate of the same material meshed with $15 \times 15 \times 2$ elements. (○) Values obtained with the DD code for a capped layer of thickness $2H$ (Gómez-García et al., 1999). (□) Other simulated values for a capped layer, replotted from Schwarz and Tersov (1996). The full line is drawn as a guide to the eye.

in the previous section and the interface is a (0 0 1) plane, perpendicular to the slip plane of the segment. This simplified geometry allows performing comparisons with other estimates reported in the literature (cf. Fig. 7). Indeed, in such a configuration, the boundary conditions at the free surface are such that the critical stress should be nearly the same as that for a capped layer of thickness $2H$ (corresponding to $2H \approx \ell$ and $\beta \approx 1$ in Eq. (4)). Such confinement effects become complex with more realistic geometrical configurations and when additional internal stresses, like misfit and elastic incompatibility stresses, are taken into account (Lemarchand et al., 2000).

The piling-up of dislocations against an impenetrable grain boundary induces another type of size effect, the dependence of the yield stress of a polycrystal on the inverse square root of the grain size, i.e., the well-known Hall–Petch law. This dependence can be modeled in terms of dislocation pile-ups (Friedel, 1964). The number n of dislocations that can pile-up in a grain of diameter d is proportional to d and to the resolved applied stress τ_a: $n \propto d\tau_a$. By an argument of virtual work, it is possible to show that the tip of the pile-up exerts a stress $\tau_p = n\tau_a$ at the boundary. When this stress concentration reaches a critical value $\tau_p = \tau_g$, where τ_g is a material constant, plastic strain is transmitted from one plastically active grain to neighboring inactive grains. Since $\tau_g \propto d\tau_a^2$, it follows that $\tau_a \propto d^{-1/2}$.

A check of the pile-up configuration leading to these stress concentration effects has been performed and is briefly sketched here. Five straight edge dislocations of same Burgers vector [0 1 0] and line direction [1 0 0] were introduced under stress in the (0 0 1) central slip plane of a simulated copper crystal. In this plane, an impenetrable wall has been introduced in order to block dislocation motion. The model crystal, of dimension $2.6 \times 15 \times 15\ \mu m^3$, was strained with a constant displacement rate until the

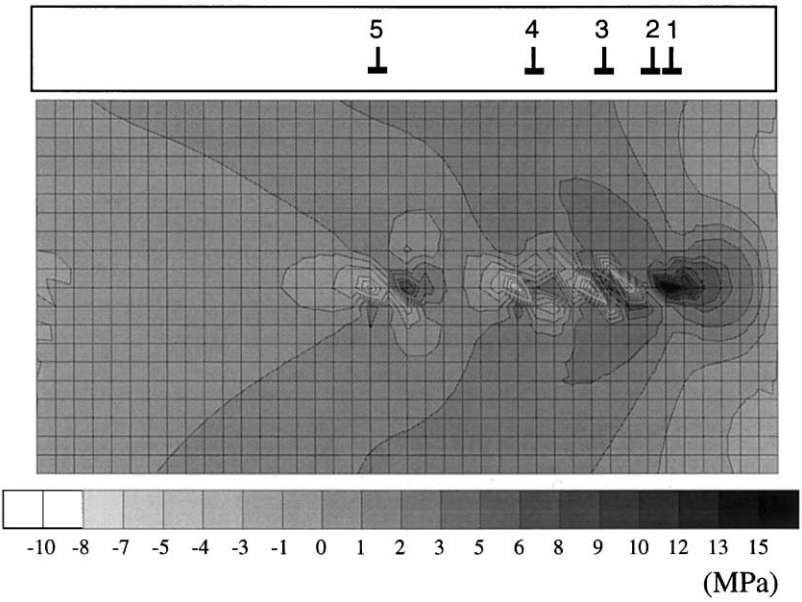

Fig. 8. Simulation of a dislocation pile-up using the MDC. (100) views, perpendicular to the dislocation lines. The trace of the (0 0 1) slip plane is horizontal. Top: The dislocation 1, at the tip of the pile-up is blocked against an impenetrable wall. The total length of the pile-up is 5.6 μm. Bottom: Isovalues of the resolved stress field in the (100) plane, showing the stress concentration on dislocation 1. Only a portion of the simulated crystal is shown.

dislocations reached an equilibrium configuration with a prescribed total pile-up length ($d = 5.6$ μm in Fig. 8). The dimension of the mesh elements along the direction of motion of the dislocations was adjusted to be of same order as the expected smallest approach distance of the first two dislocations at the tip of the pile-up (0.38 μm).

The simulated configuration and the resolved stress in the (0 0 1) central plane normal to the dislocation lines are shown in Fig. 8. This configuration was compared to a theoretical configuration computed for infinite dislocation lines in an infinite crystal. For this purpose one has to solve five equilibrium conditions for the dislocation lines, taking into account that the sum of the dislocation spacings is d, the pile-up length. This yields 6 unknown quantities, viz., 4 dislocation spacings, the applied stress τ_a and a reaction $-\tau_p$ from the wall on the leading dislocation at the pile-up tip. The computed and simulated solutions are in fair agreement. For instance, the MDC yields $\tau_p = 12.3$ MPa, whereas $\tau_p = 12.53$ MPa for the computed solution, and the distance between the first two dislocations in the pile-up is the same in both cases (0.38 μm). Thus, the adaptation of the mesh element dimension to the smallest spacing between dislocations again ensures the quality of the result. As the piled-up configurations are well reproduced, this leads to the possibility of simulating the Hall–Petch behavior of small grain aggregates.

6. Concluding remarks

The discrete-continuum method described here solves equilibrium and compatibility conditions in a dislocated material containing interfaces and/or under complex loading. Its main advantage is that it does not make use of analytical forms for the displacement fields of the dislocation segments, nor involves an $O(N^2)$ computation of their pair elastic interactions. In the DCM, one only has to estimate the amount of shear associated with dislocation motion, which is a measure of the local plastic strain. As dislocation-related length scales are underlying the continuum frame, a proper treatment of the elastic properties of the dislocation lines and of size effects can be carried out. In physical terms, the most fundamental of these length scales is the Burgers vector of the dislocations.

The price to pay for these advantages, is that one has to treat and homogenize singularities inside the simulated volume. In the present state of the DCM, it is not possible to have a correct treatment of more than one dislocation per mesh element, due to the breakdown of the interpolation procedure at short distance. In the examples presented in the previous section, the mesh size has then to be refined down to a value that is typically the smallest distance between interacting segments. This introduces a drastic limitation to the dimension of the simulated configurations. Reintroducing into the mesoscopic component of the hybrid code the explicit dislocation–dislocation interactions at short distance (smaller than the linear dimension of a mesh element) is obviously the next step to be performed.

Finally, one may divide the range of application of dislocation dynamics simulations into three sub-domains. Simple DD simulations are reasonably suited for the study of dislocation microstructures and strain hardening in single crystals. Hybrid simulations like the DCM seem to be restricted to the simulation of plastic properties in submicronic configurations that do not involve large numbers of dislocations (although the density can be very high). Large scale studies on representative volumes of structural materials containing internal interfaces appear to be out of reach for the moment.

References

Acharya, A., Bassani, J., 2000. Lattice incompatibility and a gradient theory of crystal plasticity. J. Mech. Phys. Solids 48, 1565–1595.

Aifantis, E.C., 1984. On the microstructural origin of certain inelastic models. Trans. ASME J. Eng. Mat. Technol. 106, 326–330.

Bathe, K.J., 1996. Finite Element Procedures. Prentice-Hall, Upper Saddle River, NJ.

Cleveringa, H.H.M., Van der Giessen, E., Needleman, A., 1997a. Comparison of discrete dislocation and continuum plasticity predictions for a composite material. Acta Mater. 45, 3163–3179.

Cleveringa, H.H.M., Van der Giessen, E., Needleman, A., 1997b. A discrete dislocation analysis of residual stresses in a composite material. Philos. Mag. A 79, 893–920.

Cuitiño, A.M., Ortiz, M., 1992. Computational modelling of single crystals. Modelling Simulation Mater. Sci. Eng. 1, 225–263.

Devincre, B., 1995. Mesoscale simulation of dislocation dynamics. In: Kirchner, H. et al. (Eds.), Computer Simulation in Materials Science. Kluwer, Dordrecht, Netherlands, pp. 309–323.

Devincre, B., Condat, M., 1992. Model validation of a 3D simulation of dislocation dynamics: discretization and line tension effects. Acta Metall. Mater. 40, 2629–2637.

Devincre, B., Kubin, L.P., 1997. Mesoscopic simulations of dislocations and plasticity. Mater. Sci. Eng. A 234–236, 8–14.

Eshelby, J.D., 1966. A simple derivation of the elastic field of an edge dislocation. British J. Appl. Phys. 17, 1131–1135.

Estrin, Y., 1996. Dislocation-density-related constitutive modeling. In: Krauz, A.S., Krauz, K. (Eds.), Unified Constitutive Laws of Plastic Deformation. Academic Press, New York, pp. 69–105.

Fivel, M.C., Canova, G.R., 1999. Developing rigorous boundary conditions to simulations of discrete dislocation dynamics. Modelling Simulation Mater. Sci. Eng. 7, 753–768.

Fivel, M., Robertson, C., Canova, G.R., Boulanger, L., 1998. Three-dimensional modeling of indent-induced plastic zone at a mesoscale. Acta Mater. 46, 6183–6194.

Fleck, N.A., Muller, G.M., Ashby, M.F., Hutchinson, J.W., 1994. Strain gradient plasticity: theory and experiment. Acta Metall. Mater. 42, 475–487.

Friedel, J., 1964. Dislocations, Pergamon Press, Oxford, p. 260.

Gómez-García, D., Devincre, B., Kubin, L., 1999. Dislocation dynamics in confined geometry. J. Comput. Aided Mater. Des. 6, 157–164.

Kroupa, F., 1994. Short range interaction between dislocations. Key Eng. Mater. 97–98, 377–382.

Kubin, L.P., Devincre, B., 1999. From dislocation mechanisms to dislocation microstructures and strain hardening. In: Bilde-Sørensen, et al. (Eds.), Deformation Induced Microstructures: Analysis and Relation to Properties. Risø National Laboratory, Rosklide, Denmark, pp. 61–83.

Lemarchand, C., Devincre, B., Kubin, L.P., Chaboche, J.-L., 1999. Coupled meso-micro simulations of plasticity: validation tests. In: Bulatov, V., et al. (Eds.), Multiscale Modelling of Materials. MRS Symposium Proceedings, Vol. 538. Material Research Society, Warrendale, PA, pp. 63–68.

Lemarchand, C., Devincre, B., Kubin, L.P., Chaboche, J-L., 2000. Dislocations and internal stresses in thin films: a discrete-continuum simulation. In: Lassila, D., et al. (Eds.), Multiscale Modelling of Materials, Experiments and Simulations. MRS Symposium Proceedings, Vol. 578. Materials Research Society, Warrendale, PA, pp. 87–92.

Mura, T., 1993. Micromechanics of Defects in Solids, 2nd Revised Edition. Kluwer Academic Publishers, Dordrecht, Netherlands.

Saada, G., Shi, X.L., 1995. Description of dislocation cores. Czechoslovak J. Phys. 45, 979–989.

Schwarz, K.J., Tersov, J., 1996. Interaction of threading and misfit dislocations in a strained epitaxial layer. Appl. Phys. Lett. 69, 1220–1222.

Tabourot, M., Fivel, M., Rauch, E., 1997. Generalised constitutive laws for f.c.c. single crystals. Mater. Sci. Eng. A234–236, 639–642.

Verdier, M., Fivel, M., Groma, I., 1998. Mesoscopic scale simulation of dislocation dynamics in fcc metals: principles and applications. Modelling Simulation Mater. Sci. Eng. 6, 755–770.